CARBON 46 (2008) 806–817

available at www.sciencedirect.com

ScienceDirect

journal homepage: www.elsevier.com/locate/carbon

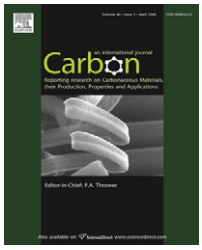

Improved thermal conductivity for chemically functionalized exfoliated graphite/epoxy composites

Sabyasachi Ganguli[a,*], *Ajit K. Roy*[a], *David P. Anderson*[b]

[a]AFRL, 2941 Hobson Way, Dayton, OH 45433, USA
[b]UDRI, 300 College Park, Dayton, OH 45469, USA

ARTICLE INFO

Article history:
Received 28 September 2007
Accepted 9 February 2008
Available online 15 February 2008

ABSTRACT

Chemically functionalized exfoliated graphite-filled epoxy composites were prepared with load levels from 2% to 20% by weight. The viscosities of the composites having load levels >4% by weight were over the processing window for the vacuum-assisted resin transfer molding process. Wide-angle X-ray diffraction revealed a rhombohedral carbon structure in the filler. Enhanced interaction between the epoxy and the graphite filler was evidenced by an improvement in the rubber modulus for the chemically functionalized graphite/epoxy composites. The thermal and electrical properties of the nanoparticle-filled epoxy composites were measured. The electrical property of the chemically functionalized graphite/epoxy composite deteriorated. Thermal conductivity of the chemically functionalized graphite/epoxy composite, however, increased by 28-fold over the pure epoxy resin at the 20% by-weight load level, increasing from 0.2 to 5.8 W/m K.

1. Introduction

The quest for improvement of thermal conductivity in aerospace structures is gaining momentum. This is even more important as modern day aerospace structures are embedded with electronics which generate considerable amounts of heat energy. This generated heat, if not dissipated, might potentially affect the structural integrity of the composite structure. The use of polymer-based composites in aerospace applications has also increased due to their obvious superior specific properties, but the thermal conductivity of the polymer matrix is very low and not suited for the thermal design loads in many aerospace applications. Several research studies have been conducted to improve the thermal conductivity of the polymeric composites. Different fillers have been used to improve the thermal conductivity of the polymeric matrix [1–15]. Fillers may be in the form of fibers or in the form of particles uniformly distributed in the polymer matrix. The thermophysical properties of fiber-filled composites are anisotropic, except for the very short, randomly distributed fibers; while the thermophysical properties of particle-filled polymers are isotropic. Numerous studies have also been conducted in recent years, where nanoparticles have been dispersed in the polymeric matrix to improve the thermal conductivity. Putnam et al. [14] used the 3ω method to study the thermal conductivity of composites of nanoscale alumina particles in polymethylmethacrylate (PMMA) matrices in the temperature range 40–280 K. It was observed that the addition of 10% by weight of 60 nm alumina particle filler decreased the thermal conductivity of the composite. Kuriger and Alam [7] studied the thermal conductivity of aligned, vapor-grown carbon fiber-reinforced polypropylene composite. They measured thermal conductivity with a laser flash instrument in the longitudinal and transverse directions for 9%, 17% and 23% fiber reinforcements by volume. The values of thermal conductivity as reported by them were 2.09, 2.75, 5.38 W/m K for the longitudinal direction and 2.42, 2.47, 2.49 W/m K for the transverse direction, respectively, while the thermal

* *Corresponding author:* Fax: +1 937 656 4706.
E-mail address: Sabyasachi.ganguli@wpafb.af.mil (S. Ganguli).
0008-6223/$ - see front matter
doi:10.1016/j.carbon.2008.02.008

conductivity of unfilled polypropylene was 0.24 W/m K. Exfoliated graphite platelets are another filler material of promise for improving the thermomechanical properties of the polymeric matrix. Aylsworth [16,17] developed and proposed exfoliated graphite as a reinforcement of polymers in 1910s. Lincoln and Claude [9] in 1980s proposed the dispersion of intercalated graphite in polymeric resins by conventional composite processing techniques. Since that time, research has been conducted on exfoliated graphite-reinforced polymers using graphite particles of various dimensions and a wide range of polymers. Kalaitzidou et al. [6] have demonstrated the use of exfoliated graphite platelets to enhance the thermal and mechanical properties of polymeric resins. They concluded that composites made by in situ processing have better mechanical properties compared to composites made by melt-mixing or other ex situ fabrication methods due to better dispersion, prevention of agglomeration and stronger interactions between the reinforcement and the polymer. Debelak and Lafdi [3] dispersed exfoliated graphite flakes in an epoxy resin and studied the thermal and electrical properties of the composites. A 24-fold increase in thermal conductivity was reported for the 20% graphite flake composite compared to the pure resin. Ma et al. [18] studied the effects of silane functionalization of multiwall carbon nanotubes on properties of CNT/epoxy composites. Their results indicated that grafting silane molecules onto a nanotube surface improved dispersion of the nanotubes in the epoxy matrix, thereby improving the interfacial interactions. These improved interfacial interactions resulted in improved mechanical and thermal properties. The study reported a decrease in electrical properties due to wrapping of the insulative silane molecules on the tubes. With respect to the prior work reviewed above, in this study we chemically treat the graphite flakes to make them compatible with the epoxy system and study the thermal, electrical and flow properties of the resultant composites. The thermal conductivity measurements performed in this study were by the laser flash diffusivity method. The laser flash method used to determine thermal property in this study has and is being used widely in the literature [19–28]. The studies reviewed [3,7] also used the same technique to determine thermal conductivity. Especially, Debelak and Lafdi [3] worked on a very similar system and the same measurement technique. Their results have been compared to the ones from our study.

2. Experimental

Exfoliated graphite (EG) flakes were supplied by Graftech International Ltd., Parma, OH. The expansion of the natural graphite flakes was performed at Graftech International, according to the following procedure. Natural crystalline graphite flakes were intercalated by acid treatment. The EG was then prepared by expanding the intercalated compound by thermal shock at 600 °C in a furnace. At this high temperature, intercalates trapped within the graphite layers decompose and expand the graphite layers. The lateral dimensions of the graphite flakes were 3.9 μm with a thickness varying between a couple of nanometers to 100 nm (data supplied by Graftech). Epon 862/Epicure W was chosen as the model system for this study. Epon 862 is an epoxy bisphenol F resin and Epicure W is an aromatic amine curing agent. An accelerating agent, Epicure 537, composed of organic salts was used to accelerate the curing reaction. Use of an accelerator in the curing reaction helped in "locking in" the dispersed morphology by enhancing the rate of the curing reaction. A typical epoxy curing reaction scheme is shown in Fig. 1.

The nanoparticles were dispersed in the epoxy using a Flacktek Speedmixer. The FlackTek SpeedMixer DAC 400 FV (Z) works by the spinning of a high-speed mixing arm at speeds up to 2750 rpm in one direction, while the basket rotates in the opposite direction. This combination of forces in different planes enables incredibly fast mixing. Thermal conductivity of the synthesized composites was measured by a Netzsch LFA 457 laser flash thermal diffusivity apparatus. Thermomechanical properties of the specimens were measured using a TA Instruments DMA 2980. Viscosity of the pure and composite resin systems was measured by a Rheometrics, Inc. ARES rheometer in the parallel plate mode. Wide-angle X-ray measurements were obtained for the EG nanoparticles to determine the change in *d*-spacing due to processing. The solid composite samples were cut to expose an inside surface; each sample was mounted such that the front face was held at the Bragg–Brento diffracting position. The X-ray diffraction (XRD) was obtained on a Rigaku DMAX B horizontal diffractometer in a symmetric theta-two theta reflective mode. The Cu Kα radiation was produced using a rotating anode generator at 40 kV and 150 mA with a diffracted beam monochromator. The peak location and widths were determined using PeakFit™ software. Electrical properties were measured by a 4-point conductivity probe acquisition system manufactured by Agilent Technologies, Inc. The distance between the pins was fixed at 2.54 mm. Typical specimen dimensions for the conductivity experiments were 25 mm × 3 mm × 0.1 mm.

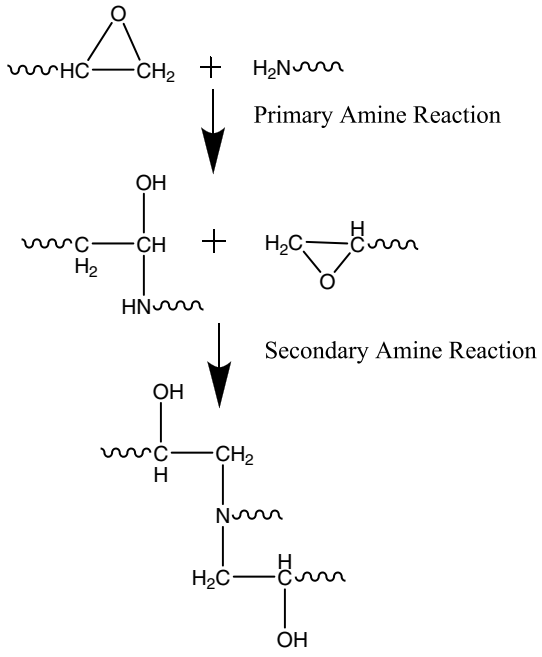

Fig. 1 – Typical epoxy-amine curing reaction scheme.

2.1. *Chemical modification of the exfoliated graphite flakes*

The grafting reaction was carried out in a mixture of water/ethanol (25/75 by volume). A quantity of 3 g of γ-APS (3-aminopropoxyltriethoxy silane) was first introduced into 1000 ml of the mixture of water/ethanol, and the temperature was kept at 80 °C. Then 10 g of exfoliated graphite were added into the above-mentioned solution, and the grafting reaction was realized, under shearing, for 5 h at 80 °C. The reaction product was filtered and washed six times using a mixture of H_2O/ethanol and freeze dried. The resultant product was ground and placed in a sealed container for characterization. The size of the graphite flakes after the grinding operation was not determined. X-ray photoelectron spectroscopy (XPS) of the grafted graphite flakes was performed to verify the grafting of the amine groups on the graphite flakes.

Compositional analyses were made with an XPS system operated at a pressure of 8×10^{-10} torr. Binding energy positions were calibrated using the Au $4f_{7/2}$ peak at 83.93 eV and the Cu 3s and Cu $2p_{3/2}$ peaks at 122.39 and 932.47 eV_0. The results of the XPS study are presented in Figs. 2 and 3. Fig. 2 shows the C1s spectrum for the as-received exfoliated (exfoliated by Graftech International) graphite flakes. The C1s peak can be deconvoluted into four fitting curves. We observe peaks at 284.18, 285.28, 286.1 and 286.7 eV. The respective percentages are presented in Table 1. Evidence of –COO, –C=O and C–O bonds in the C1s spectrum may be attributed to the oxidation of the graphite flakes as a result of the treatment with strong acids during the exfoliation procedure. The atomic compositions of the as-received oxidized graphite flakes are presented in Table 2.

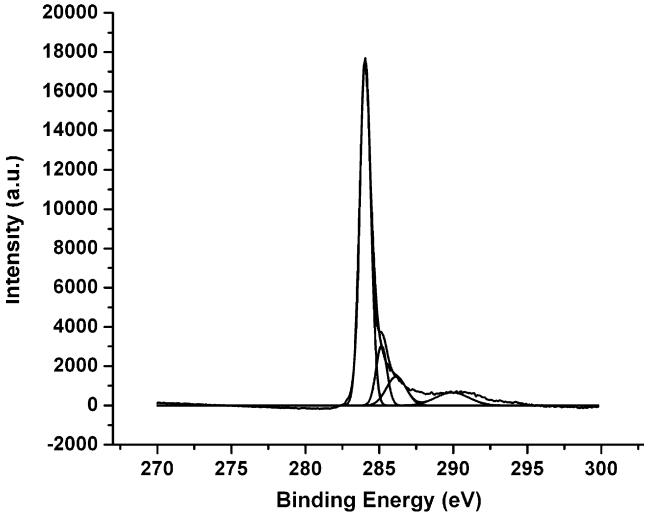

Fig. 2 – C1s spectrum for the exfoliated graphite flakes.

The C1s spectrum and N1s spectrum for the silane modified graphite flakes are presented in Fig. 3. The C1s spectrum for the amine silane modified graphite flakes showed a similar spectrum to the unmodified one; however, a new peak attributed to Si–C appeared at 282.8 eV with an elemental composition of silicon at 3.4%. The Si–C peak confirms the presence of the silane on the graphite flakes after the treatment with the amine silane. The C1s spectrum for the silane-modified graphite flakes may be deconvoluted into six peaks at 282.8, 284.18, 285.16, 286.2, 287.78 and 289.2 eV. The respective percentage compositions of the individual peaks are presented in Table 1. From Table 1 we determine that the peak at 284.18 eV is attributed to elemental carbon (sp^2). The N1s spectrum for the modified graphite flakes presented in Fig. 3 can be deconvoluted into two peaks at 399.8 and 402.4 eV, respectively. The predominant peak at 399.8 eV is attributed to a compound of nitrogen, silicon, carbon and oxygen. The Si 2p spectrum for the silylated graphite flakes is presented in Fig. 4. The Si 2p peak can be deconvoluted into two peaks. The first one at 101.6 eV represents the bonding between silicon with oxygen. The second peak at 103.3 eV may be attributed to the siloxane resulting from hydrolysis of the amine silane molecule as part of the silylation reaction. The N1s peak shows the presence of protonated amine at 399.8 eV resulting from the chemisorption of the amine silane. A schematic of the reaction scheme for the silylation of the graphite flakes is presented in Fig. 5. The electron-rich nitrogen present in the amino silane enters into hydrogen bonding interactions with the hydrogen donating oxidized carbon group on the graphite surface created by the acid

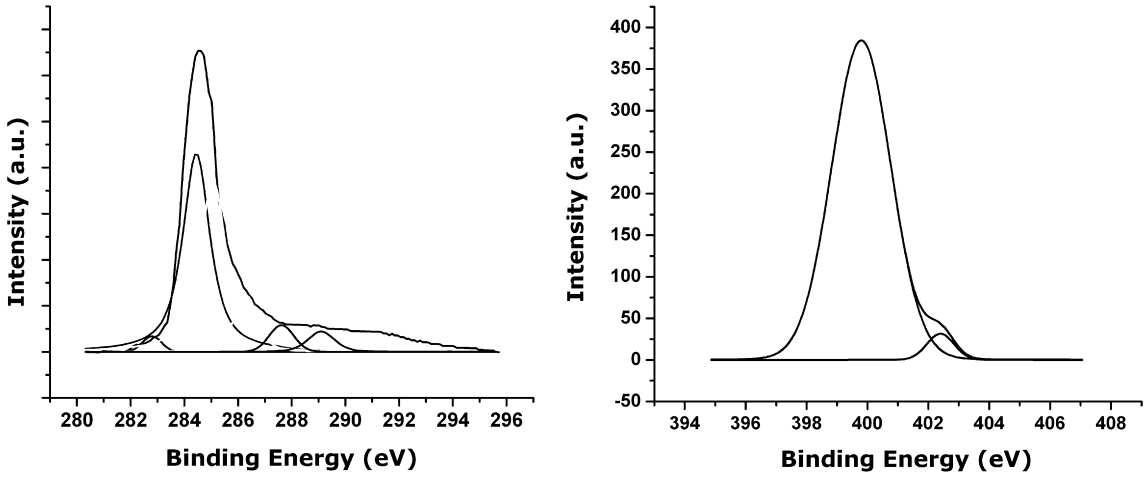

Fig. 3 – C1s and N1s spectrums for the silanized graphite flakes.

Table 1 – Summary of the relative percentage of the carbon and respective assignation

Binding energy (eV)	Si–C	C_g sp^2	C_d sp^3	C–O	–C=O	CO–O
	282.8	284.18–284.5	285.1–285.3	286–286.5	287.6–287.8	289–289.4
Oxidized	0	74.2	4.4	8.1	0	13.3
Silylated	3.4	65.7	5.2	11	4.9	9.8

Table 2 – Summary of the elemental composition

Element (atom %)	C	O	N	Si
Oxidized	94.35	5.65	0.0	0.0
Silylated	83.89	10.5	2.31	3.3

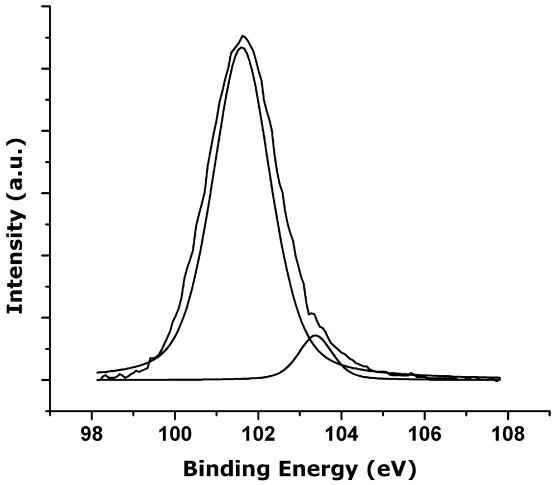

Fig. 4 – Si 2p XPS spectrum of silanized graphite flakes.

treatment. It is assumed that amino groups of the chemisorbed graphite flakes (due to silane coupling agent APS) react with the epoxy moieties of the resin in a manner similar to the reaction between epoxy and an amine-based hardener in the bulk phase.

2.2. *Processing and characterization of composites*

Differential scanning calorimetry (DSC) helped to determine the amount of accelerator to be used and also to identify the processing window for dispersion of the nano-constituents in the resin. DSC scans were run on ~10 mg samples enclosed in hermetically sealed Al pans. The samples were heated from room temperature to 300 °C at a 5 °C/min heating rate. The DSC scans are shown in Fig. 6. The crosslinking reaction of the epoxy curing is characterized by an exotherm peak in the DSC heat flow curve. The onset point of the exotherm corresponds to the gelling or the onset of the first crosslinking. At that point the morphology gets "locked-in". Thus the processing window has to be chosen at a temperature below the gel-point of the thermoset polymer. Based on the DSC scans, it was determined that the dispersion could be carried out at 60 °C with 3% accelerator without the risk of starting the curing reaction. In order to test this, an isothermal DSC experiment at 60 °C was performed. It was observed that there was no evidence of initiation of the epoxy curing reaction at 60 °C even after 120 min. The mixing protocol for the synthesis of all the composites was as follows – Epon 862 and fillers are mixed in the Flacktek mixer at 2800 rpm for

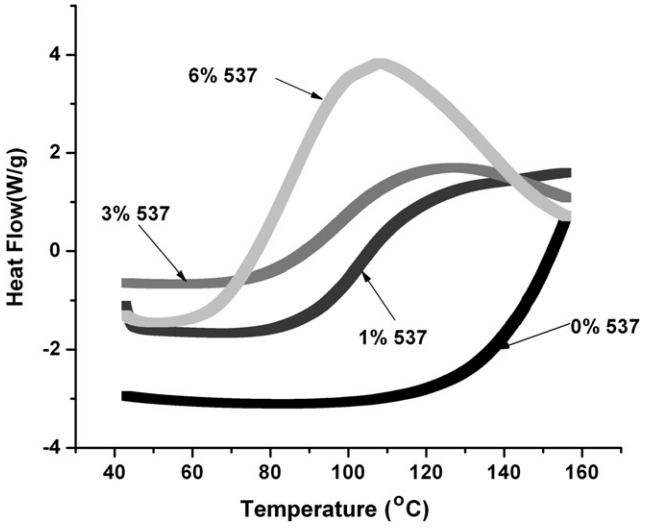

Fig. 6 – DSC scans to determine optimal processing window.

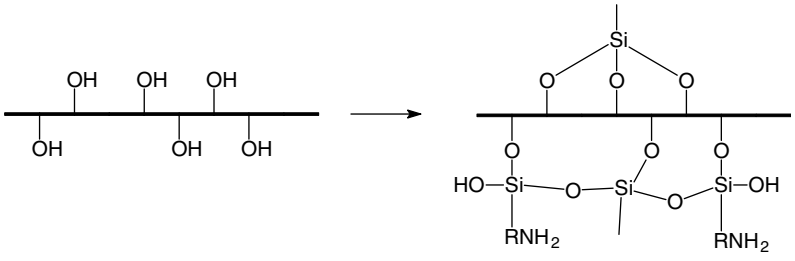

Fig. 5 – Schematic of the silane treatment of the graphite flakes.

8 min. Subsequently, the Epicure W along with the Epicure 537 was mixed at 1000 rpm for 30 s. Two sets of specimens, one with as supplied graphite flakes (EXF) and the other with chemically treated graphite flakes (FN) were synthesized. The loading levels of the graphite platelets were 2, 4, 8, 16 and 20 wt% of the epoxy resin.

2.3. *Rheology of the composites*

Rheology of the composites was performed on an advanced rheometrics expansion system (ARES) equipped with a forced convection oven. ARES is a mechanical spectrometer that is capable of subjecting a sample to either a dynamic or steady shear strain deformation and then measuring the resultant torque expended by the sample in response to this shear strain. Shear strain is applied by the motor, and the torque is measured by the transducer. For a set strain amplitude and frequency, actual sample deformation is determined by the measured motor and transducer displacement. The flow properties of the composites were measured in a parallel plate mode at an angular frequency of 6.28 Hz. The strain exerted on the specimens was 3%, and the temperature range investigated was 35–250 °C at 5 °C/min. In order for a polymer to qualify for vacuum-assisted resin transfer molding (VARTM), the viscosity has to be less than 3000 cP. The processing window for polymers is the range of temperature over which the viscosity remains in the processing regime. The results of the rheology test are presented in Fig. 7. We observe from the rheology plot that the pure polymer has a viscosity of ~32 cP at 75 °C. Composites formulated of the unfunctionalized graphite exceed this viscosity range for any loading level above 2 wt%. For the functionalized graphite the 2 wt% and the 4 wt% fall within the processing window of the VARTM process. The functionalized graphite-based composites perform better than the unfunctionalized ones in this figure of merit. Both the 2 and 4 wt% functionalized composites have a longer processing window than the 2 wt% unfunctionalized graphite composites. The addition of graphite flakes in the epoxy matrix increases the viscosity of the dispersions at all loading levels for both the functionalized and the unfunctionalized systems. This may be due to reduction of free volume in the system giving rise to steric hindrance. The difference in viscosity profile between the functionalized and unfunctionalized systems at low filler level may be due to the fact that thermodynamically the reaction between the epoxy and the amine is preferred at the bulk phase than between the functionalized graphite flakes and the epoxy resin. This explains why the viscosity remains nearly invariant at lower temperatures for the 4% functionalized system. After the formation of bonds in the bulk phase, at elevated temperatures, reaction ensues between the functionalized graphite flakes and the epoxy matrix and the viscosity increases rapidly resulting in a totally crosslinked system.

2.4. *Curing of the epoxy resin composites*

The composites were cured as follows – heat at 3 °C/min to 120 °C, hold for 30 min under 30 in. vacuum, followed by heat at 3 °C/min to 177 °C/min and hold for 2 h.

3. Results and discussions

3.1. *Thermomechanical properties*

The thermomechanical properties of the synthesized composites were measured by a TA DMA 2980 at 1 Hz frequency, 10 μm amplitude. The temperature range at which the samples were evaluated was 35–225 °C, and the heating rate was 5 °C/min. The tan δ plots for the unmodified graphite platelet composites are presented in Fig. 8. The peak of the tan δ curve provides the glass transition temperature (T_g) of the polymer. We observe that the T_g of the pure epoxy resin is about 155 °C. With the addition of 2% and 4% untreated exfoliated graphite platelets, the T_g rises to about 165 °C. With a further 4% addition of the graphite platelets, the T_g rises to 175 °C. The rise in T_g in any polymeric system is associated with a restriction in molecular motion, reduction in free volume and/or higher degree of crosslinking. In this case it is most likely that the

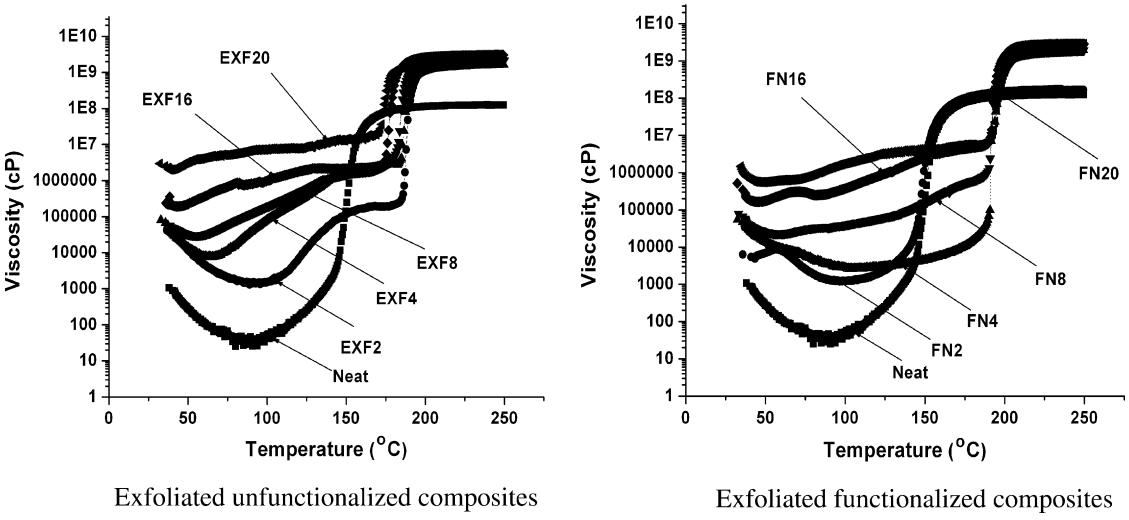

Fig. 7 – Viscosity profiles for the unfunctionalized and functionalized graphite composites.

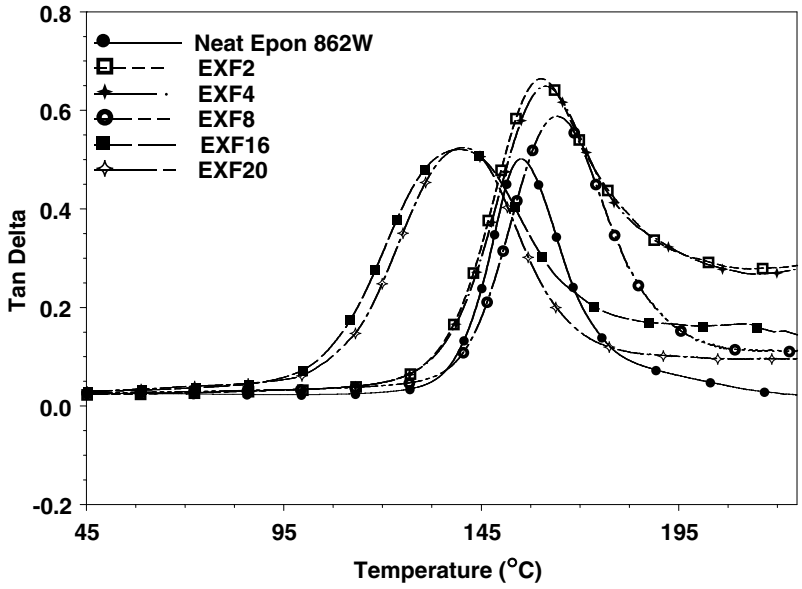

Fig. 8 – Tan δ plots for the untreated exfoliated graphite–epoxy composites.

graphite platelets restrict the molecular motions and also reduce the free volume, thereby restricting the motion of the epoxy molecule. This results in the rise in the glass transition temperature of the composites. At 20% graphite platelet loading, the T_g drops drastically. This may be due to phase separation/agglomeration of the graphite platelets. Thus it seems there is an optimum graphite platelet loading level above which the platelets re-agglomerate.

The tan δ plots for the chemically treated graphite platelet composites are presented in Fig. 9. A 7% rise in the T_g is observed for the 2%, 4% and 8% composite. As observed for the untreated graphite platelet composites, a decrease in T_g is observed for the higher loading levels of the chemically treated graphite platelet composites. This may be attributed to formation of agglomerations as observed for the untreated composites.

The storage modulus plots for the exfoliated and silylated graphite composites are presented in Figs. 10 and 11, respectively. The "rubbery plateau" of the storage modulus is an indication of the degree of interaction between the polymeric system and the fillers. We observe that the rubbery modulus steadily increases with increasing filler content for both systems. At 20% loading level, the rubbery modulus for the silylated graphite composites is ~240 MPa, while that for the exfoliated graphite composites is ~100 MPa. This enhancement in the rubbery modulus is directly correlated to the chemical bonding of the silylated graphite flakes to the epoxy network.

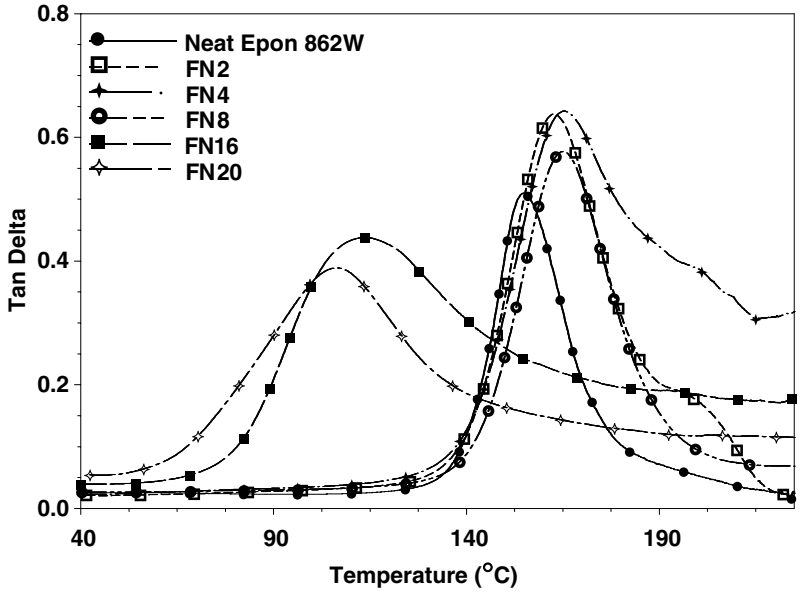

Fig. 9 – Tan δ curves for the functionalized graphite/epoxy composites.

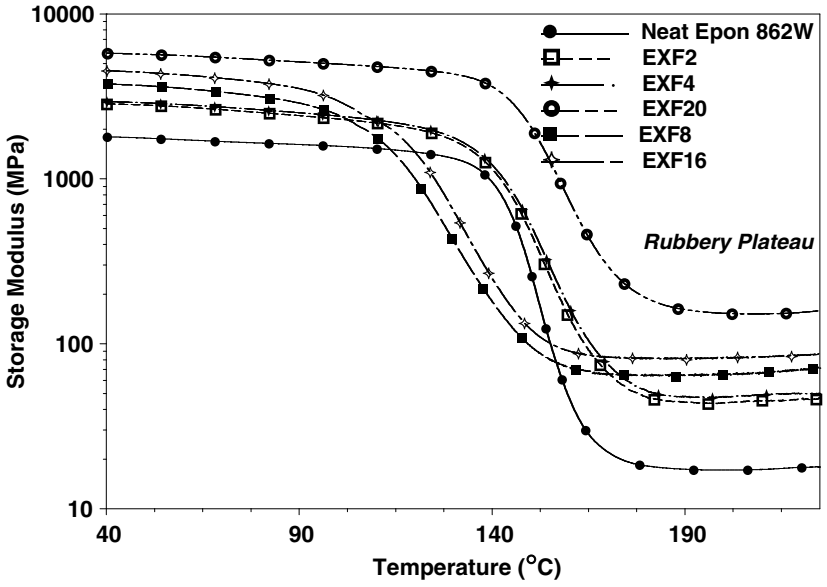

Fig. 10 – Storage modulus curves for exfoliated untreated graphite/epoxy composites.

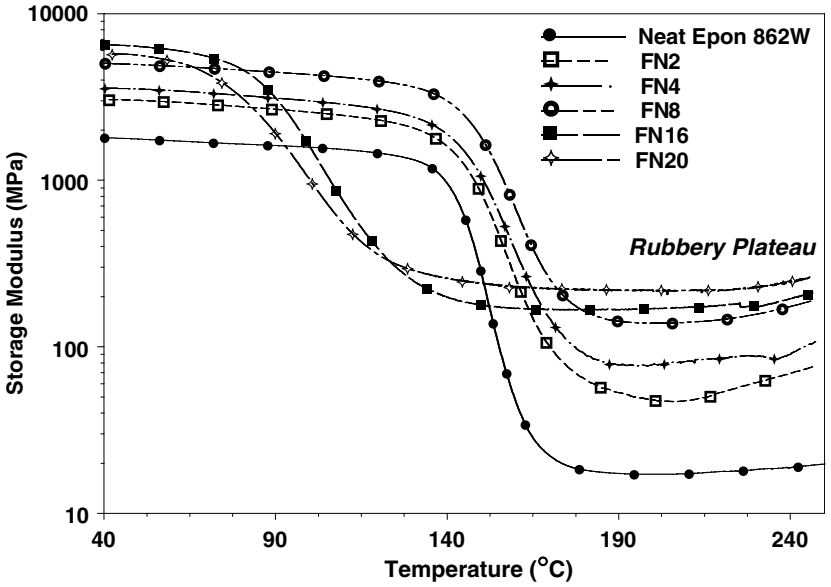

Fig. 11 – Storage modulus curves for exfoliated chemically treated graphite/epoxy composites.

3.2. *Morphology*

3.2.1. WAXD

XRD was performed on a number of epoxy composite samples with varying amounts of graphite flakes added. Both flakes that were exfoliated (Exf) and exfoliated and then functionalized (FN) were examined. Fig. 12 shows a series of patterns for the exfoliated flakes showing an increase in the crystalline graphitic content as the amount of flakes was increased (the patterns normalized to give the same amount of amorphous epoxy scattering).

One can observe several extraneous peaks in Fig. 12 not normally observed in graphite. Some of the peaks are only observed in very highly graphitic samples, and other peaks were traced to an abundance of rhombohedral graphite. Normal hexagonal (2H) graphite has alternating graphene layers in an ABABAB stacking sequence. Off-axis reflections (hkl) are only observed in 3D graphite, and many are observed as indicated in Table 3. The extraneous peaks were first reported by Lipson and Stokes [29]. A small amount of rhombohedral (3R) graphite exists in natural graphite due to a stacking defect producing the ABCABC stacking sequence. Grinding has been known to produce more of this 3R phase [30] and is apparently present in significant amounts in the graphite flakes used in this study. Table 3 shows the experimentally observed peaks and the corresponding peaks for both hexagonal (2H) and rhombohedral (3R) graphite.

Fig. 13 shows two patterns, one from the functionalized graphite flakes and the other from the exfoliated only graphite flakes. Based on the relative heights of the peaks between

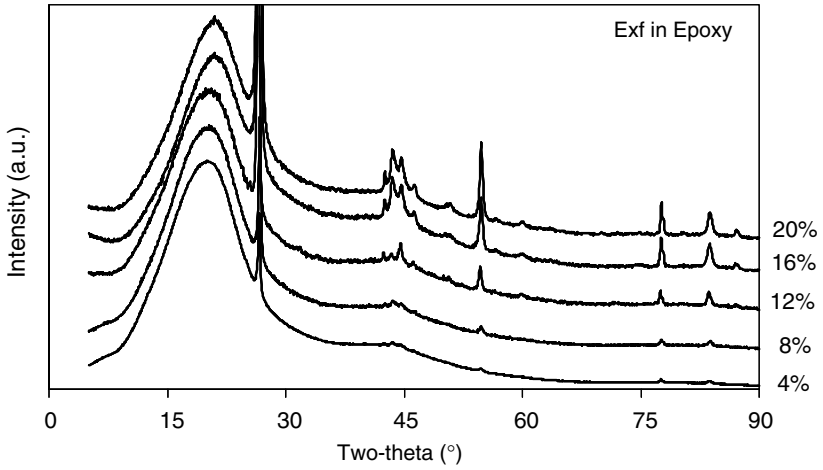

Fig. 12 – Normalized XRD patterns (horizontally offset for clarity) showing an increase in crystalline graphitic content as the flake content increases.

Table 3 – Observed XRD peak d-spacings for the graphite flake composites and comparison to expected hexagonal (2H) and rhombohedral (3R) graphite (hexagonal indexing for both)

Experimental *d*-spacing (Å)	2H			3R		
	(*hkl*)	Theory	Difference	(*hkl*)	Theory	Difference
3.355	(002)	3.375	0.020	(003)	3.348	−0.007
2.123	(100)	2.138	0.015			
2.078				(101)	2.081	0.003
2.025	(101)	2.039	0.014			
1.96				(012)	1.958	−0.002
1.796	(102)	1.807	0.011			
1.675	(004)	1.681	0.006	(006)	1.674	−0.001
1.623				(104)	1.623	0
1.54	(103)	1.547	0.007			
1.462				(015)	1.46	−0.002
1.316	(104)	1.322	0.006			
1.229	(110)	1.234	0.005	(110)	1.228	−0.001
1.194				(107)	1.19	−0.004
1.154	(112)	1.16	0.006	(113)	1.153	−0.001
1.134	(105)	1.139	0.004			
1.118	(006)	1.12	0.002	(009)	1.116	−0.002

42° and 47°, the exfoliated graphite flakes have more of the rhombohedral phase than the functionalized flakes, but both contain a significant portion. The 2H (100) peak occurs at 42.5° and the (101) at 44.7°, while the 3R (101) peak occurs at 43.5° and the (012) at 46.3°. All the flakes had graphitic *d*-spacings of ~3.355 Å with crystallite sizes greater than 300 Å. More precise crystallites sizes could not be measured due to the instrumental broadening of the diffractometer.

3.2.2. *SEM*

The microstructure of the synthesized composites were investigated by an FEI Sirion HRSEM at 10 kV accelerating voltage. All the specimens were polished prior to coating them with carbon. For each specimen two micrographs are presented – one at a relatively low magnification and one at a higher magnification. Four percent by weight graphite filler load level was chosen as the representative loading level to compare the microstructure of the EXF and FN graphite/epoxy composites. The SEM micrographs for the EG composite and the silylated EG composite are presented in Figs. 14 and 15, respectively. At the lower magnifications both micrographs show evidence of agglomerations of the graphite filler. At the higher magnifications, we observe better graphite–epoxy interactions for the silylated graphite–epoxy composite compared to the EG composite. This result corroborates well with the result from the thermomechanical study.

3.3. *Thermal conductivity*

Heat capacities and thermal conductivity of the specimens were measured by the Netzsch laser flash diffusivity system, LFA 457. The flash parameters used for this experiment were

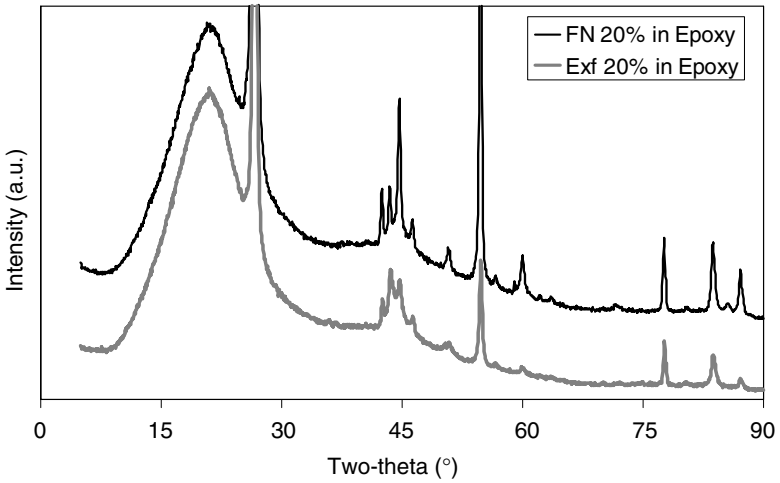

Fig. 13 – Normalized XRD patterns (horizontally offset for clarity) showing more rhombohedral graphite in the exfoliated (Exf) sample relative to the functionalized (FN) flakes.

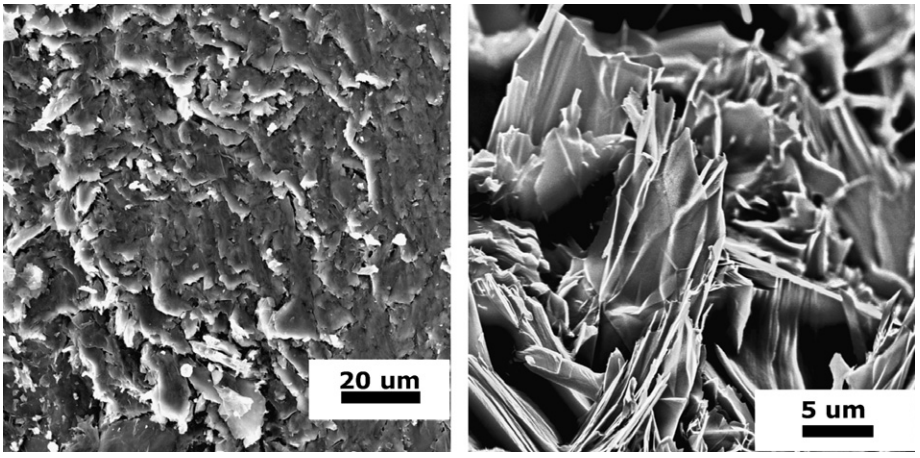

Fig. 14 – SEM micrographs of the exfoliated graphite/epoxy composite.

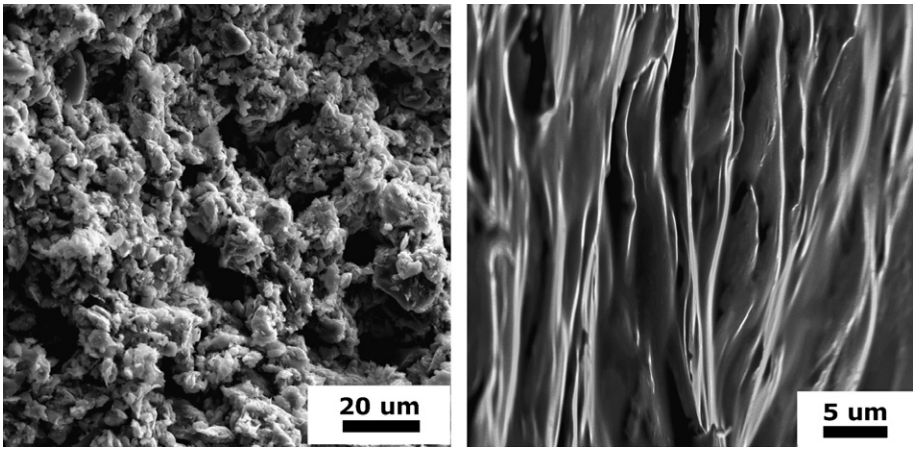

Fig. 15 – SEM micrographs of the chemically treated graphite/epoxy composite.

a laser voltage of 1922 V, 100% open filter. These laser parameters resulted in approximate laser energy of 6.13 J incident on the specimen surface. The reference used for the heat capacity calculation was a 5-mm-thick specimen of POCO graphite. The reference sample was also coated with a thin layer of graphite. This instrument and method conform to

Table 4 – Results of the thermal diffusivity experiment

Specimen	C_p (J/g K)	Diffusivity (mm^2/s)	K (W/m K)
Neat	1.060	0.157	0.195
FN2	0.966	0.267	0.303
FN4	0.966	0.384	0.443
FN8	1.000	0.993	1.235
FN16	1.000	2.644	3.268
FN20	1.177	4.152	5.864
EXF2	0.779	0.278	0.260
EXF4	0.800	0.342	0.319
EXF8	0.733	0.582	0.578
EXF16	0.801	2.459	2.267
EXF20	0.703	4.151	4.265

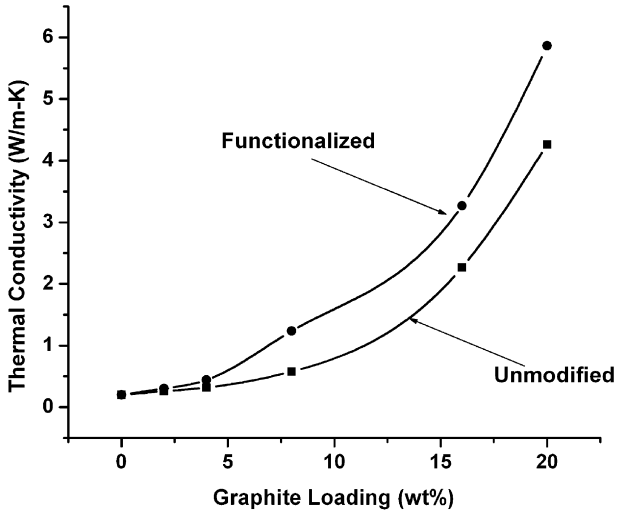

Fig. 16 – Thermal conductivity plot for the graphite–epoxy composite.

ASTM E1461-92, "Standard Test Method for Thermal Diffusivity of Solids by the Flash Method" for the measurement of thermal diffusivity.

The result of the thermal diffusivity test is presented in Table 4. The thermal conductivities of the different specimens as measured by the LFA 457 have been plotted and are reported in Fig. 16. The thermal conductivity of the pure Epon 862/W epoxy resin is around 0.2 W/m K. The thermal conductivity of the epoxy resin barely changes with the addition of 2% and 4% untreated exfoliated graphite flakes. At 8% loading, the thermal conductivity increases from 0.2 to 0.5 W/m K. As the filler concentration is further increased to 16%, the thermal conductivity increases 9-fold to ~2 W/m K. Thermal conductivity increases 19-fold compared to the pure resin (0.2 W/m K) to 4 W/m K with a filler concentration of 20%. The thermal properties of the chemically modified graphite flake composites exhibit similar behavior to the untreated composites at low filler levels (until 4% loading). At 8% filler concentration, the thermal conductivity value of the treated composites is nearly double that of the untreated composites. A similar improvement in thermal conductivity is noted for all the higher concentrations of the treated graphite flake composites. Addition of 20% treated graphite flakes in the epoxy resin increases the thermal conductivity of the epoxy resin to 5.8 W/m K – a 28-fold improvement.

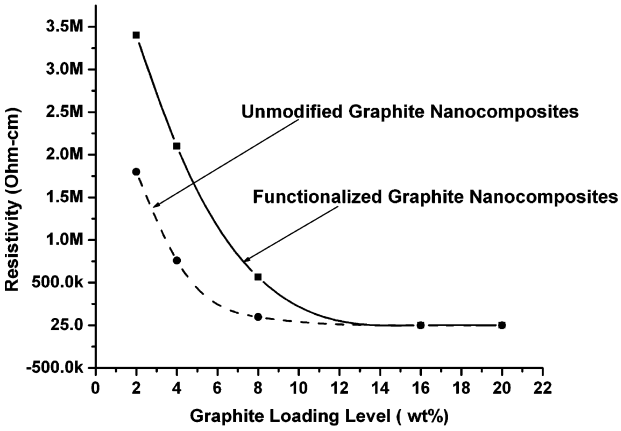

Fig. 17 – Electrical resistivity plot for the graphite–epoxy composites.

Debelak and Lafdi [3] reported thermal conductivity of exfoliated graphite–epoxy composites with graphite fillers of three different sizes. In their study, they used filler sizes of 297, 150 and 90 μm. The highest thermal conductivity achieved in that study at 20% filler loading for all the different sizes was 4.3 W/m K. That corresponds well with the thermal conductivity results of the untreated graphite composites used in this study. In comparison the silylated graphite composites at 20% loading level had a thermal conductivity of 5.8 W/m K, a 35% increase due to the silylation of the graphite flakes. The mode of thermal conduction in amorphous polymers is primarily phonons. In order to improve the overall thermal transport in filled amorphous polymeric systems, the acoustic impedance mismatch (a function of the acoustic speed and the density of the medium) at the interface between the fillers and the polymeric matrix has to be reduced. The use of functionalized graphite platelets increased thermal conductivity by minimizing interfacial phonon scattering. Functionalization seems to improve the interfacial heat transfer between the graphite platelets and the epoxy matrix. For the unfunctionalized graphite composites the acoustic impedance is higher which results in a large thermal contact resistance at the filler–epoxy interface thereby reducing the thermal conductivity of the overall system. Formation of covalent bonds between the graphite platelets and the epoxy matrix due to the chemical functionalization of the graphite platelets reduces the acoustic impedance mismatch at the interface and improves the thermal conduction in the overall composite.

3.4. *Electrical property study*

The electrical resistivity curve for the graphite/epoxy composites is presented in Fig. 17. The electrical resistivity measurements were performed by a 4-point probe technique. Epoxy resin without any conductive filler is essentially insulative with a resistivity of $1.58 \times 10^8\ \Omega$ cm.[1] As expected, addition of graphite flake decreased the electrical resistivity

[1] Product bulletin: EPON resin 862, March 2005, available from: <http://www.hexionchem.com/pds/E/EPON™%20Resin%20862.pdf>.

significantly. At 8% filler loading, the electrical resistivity for the treated composites was double that of the untreated graphite composites. The drop in the electrical resistivity for the untreated composites was significantly prominent at lower loadings for the treated graphite composites compared to the treated ones. At higher concentrations of the graphite platelets, both the treated and the untreated composites had similar electrical properties. The insulative silane molecules on the graphene sheets most probably prevent electron tunneling, thereby degrading the electrical properties of the treated composites. At lower filler concentrations the effect of the silane molecule is more prominent than at higher concentrations. At higher concentrations, due to the physical proximity of the graphite platelets, electron tunneling becomes easier, thereby making the properties comparable to the untreated graphite composites.

4. Conclusions

In the present work, the effects of silane functionalization of exfoliated graphite platelets were investigated on the thermal, electrical and thermomechanical properties of epoxy composites with different concentrations of the exfoliated graphite. Major findings from this study are:

(1) The chemically modified graphite/epoxy composites exhibited improved storage modulus than the untreated ones.
(2) Enhanced interaction at the epoxy graphite interface was evidenced by improvement in the rubbery modulus for the chemically modified graphite/epoxy composites.
(3) Decrease in glass transition temperature at higher filler loadings for both the chemically modified and unmodified graphite composites is observed. It was inferred that there is an optimum graphite platelet loading level above which the platelets re-agglomerate.
(4) XRD studies revealed the evolution of a rhombohedral structure during the exfoliation of the flakes.
(5) Electrical conductivity of the silane–graphite composites at low filler concentration deteriorated due to wrapping of the insulative silane around the graphite surface.
(6) Thermal conductivity of the surface-treated composites improved by 21-fold compared to the pure epoxy resin at 20% by weight load level.
(7) Though we achieved significant enhancements in the thermal conductivity, the viscosity of the composites at higher filler loadings also increased, rendering them outside the processing window of conventional composite processing.

REFERENCES

[1] Bagchi A, Nomura S. On the effective thermal conductivity of carbon nanotube reinforced polymer composites. Compos Sci Technol 2006;66(11–12):1703–12.
[2] Chang TE, Kisliuk A, Rhodes SM, Brittain WJ, Sokolov AP. Conductivity and mechanical properties of well-dispersed single-wall carbon nanotube/polystyrene composite. Polym J 2006;47(22):7740–6.
[3] Debelak B, Lafdi K. Use of exfoliated graphite filler to enhance polymer physical properties. Carbon 2007;45(9):1727–34.
[4] Jimenez GA, Jana SC. Oxidized carbon nanofiber/polymer composites prepared by chaotic mixing. Carbon 2007;45(10):2079–91.
[5] Jimenez GA, Jana SC. Electrically conductive polymer nanocomposites of polymethylmethacrylate and carbon nanofibers prepared by chaotic mixing. Compos Part A: Appl Sci Manuf 2007;38(3):983–93.
[6] Kalaitzidou K, Fukushima H, Drzal LT. A new compounding method for exfoliated graphite-polypropylene nanocomposites with enhanced flexural properties and lower percolation threshold. Compos Sci Technol 2007;67:2045–51.
[7] Kuriger RJ, Alam MK. Thermal conductivity of thermoplastic composites with submicrometer carbon fibers. Exp Heat Trans 2002;15(1):19–30.
[8] Lau K-T, Lu M, Liao K. Improved mechanical properties of coiled carbon nanotubes reinforced epoxy nanocomposites. Compos Part A 2006;37(10):1837–40.
[9] Lincoln VF, Claude Z. Inventors, organic matrix composites reinforced with intercalated graphite. US Patent 4,414,142; 1983.
[10] Lisunova MO, Mamunya YP, Lebovka NI, Melezhyk AV. Percolation behaviour of ultrahigh molecular weight polyethylene/multi-walled carbon nanotubes composites. Eur Polym J 2007;43(3):949–58.
[11] Liu C, Oshima K, Shimomura M, Miyauchi S. Anisotropic conductivity-temperature characteristic of solution-cast poly(3-hexylthiophene) films. Synth Met 2006;156(21–24):1362–7.
[12] Luyt AS, Molefi JA, Krump H. Thermal, mechanical and electrical properties of copper powder filled low-density and linear low-density polyethylene composites. Polym Degrad Stab 2006;91(7):1629–36.
[13] Moisala A, Li Q, Kinloch IA, Windle AH. Thermal and electrical conductivity of single- and multi-walled carbon nanotube-epoxy composites. Compos Sci Technol 2006;66(10):1285–8.
[14] Putnam SA, Cahill DG, Ash BJ, Schadler LS. High-precision thermal conductivity measurements as a probe of polymer/nanoparticle interfaces. J App Phys 2003;94(10):6785–8.
[15] So HH, Cho JW, Sahoo NG. Effect of carbon nanotubes on mechanical and electrical properties of polyimide/carbon nanotubes nanocomposites. Eur Polym J 2007;43(9):3750–6.
[16] Aylsworth JW. Expanded graphite and composition thereof. US Patent 1,137,373; 1915.
[17] Aylsworth JW. Expanded graphite. US Patent 1,191,383; 1916.
[18] Ma PC, Kim J-K, Tang BZ. Effects of silane functionalization on the properties of carbon nanotube/epoxy nanocomposites. Compos Sci Technol 2007;67(14):2965–72.
[19] Aliev AE, Guthy C, Zhang M, Fang S, Zakhidov AA, Fischer JE. Thermal transport in MWCNT sheets and yarns. Carbon 2007;45(15):2880–8.
[20] Bison PG, Marinetti S, Mazzoldi A, Grinzato E, Bressan C. Cross-comparison of thermal diffusivity measurements by thermal methods. Infrared Phys Technol 2002;43(3–5):127–32.
[21] Blumm J, Lindemann A, Min S. Thermal characterization of liquids and pastes using the flash technique. Thermochim Acta 2007;455(1–2):26–9.

[22] Cernuschi F, Lorenzoni L, Bianchi P, Figari A. The effects of sample surface treatments on laser flash thermal diffusivity measurements. Infrared Phys Technol 2002;43(3–5):133–8.
[23] dos Santos WN, Iguchi CY, Gregorio Jr R. Thermal properties of poly(vinilidene fluoride) in the temperature range from 25 to 210 °C. Polym Test [in press], doi: 10.1016/j.polymertesting.2007.10.005.
[24] Iguchi CY, dos Santos WN, Gregorio Jr R. Determination of thermal properties of pyroelectric polymers, copolymers and blends by the laser flash technique. Polym Test 2007;26(6):788–92.
[25] Min S, Blumm J, Lindemann A. A new laser flash system for measurement of the thermophysical properties. Thermochim Acta 2007;455(1-2):46–9.
[26] Nunes dos Santos W, Mummery P, Wallwork A. Thermal diffusivity of polymers by the laser flash technique. Polym Test 2005;24(5):628–34.
[27] Sun Lee W, Yu J. Comparative study of thermally conductive fillers in underfill for the electronic components. Diam Relat Mater 2005;14(10):1647–53.
[28] Xie H, Cai A, Wang X. Thermal diffusivity and conductivity of multiwalled carbon nanotube arrays. Phys Lett A 2007;369(1–2):120–3.
[29] Lipson H, Stokes AR. The structure of graphite. Proc Roy Soc London Series A 1942;181(984):101–5.
[30] Bacon GE. A note on the rhombohedral modification of graphite. Acta Crystallogr 1950;3(4):320.